

## CHAPTER VI

### Mixed-integer Self-adaptive Differential Evolution with Augmented Lagrange Multiplier Method

#### 6.1 Introduction

The chapter is started with the introduction of the mixed-integer self-adaptive differential evolution with augmented lagrange multiplier method (MISADE\_ALM) for solving the optimal power flow (OPF) problems in section 6.2. Only the sequential MISADE\_ALM is considered in this chapter. The discussion of the numerical results and conclusion are provided in sections 6.3 and 6.4 respectively.

#### 6.2 Mixed-integer SADE\_ALM based optimal power flow (MISADE\_ALM-OPF)

Similar to SADE\_ALM, the proposed mixed-integer self-adaptive differential evolution with augmented lagrange multiplier method (MISADE\_ALM) consists of two iterative loops, i.e. the inner loop and the outer loop. The inner loop solves the unconstrained minimization problem through the augmented lagrange function  $L_a$  using mixed-integer self-adaptive differential evolution (MISADE). After the unconstrained minimization problem has been solved, the outer loop will update the lagrange multipliers  $\beta$ s and the penalty parameter  $r_g$  by the ALM method to create the new augmented lagrange function  $L_a$ . The algorithm is then repeated until a termination criterion, i.e. maximum number of iterations or convergence of the optimal solution, is reached. The flowchart of the MISADE\_ALM when applied to solve the OPF problems is shown in Figure 6.1. Details of MISADE\_ALM are described as in the following.

##### 6.2.1 The inner loop iteration

The inner loop solves the augmented lagrange function  $L_a$  using mixed-integer self-adaptive differential evolution (MISADE). The algorithm of the inner loop iteration is the same as described in section 4.3.1 of chapter 4. However, there is one additional procedure to be included in MISADE for handling integer and/or discrete control variables as shown in Figure 6.1 of which it can be described as in the following.

In the canonical form of differential evolution, only continuous floating point variables can be used. However, MISADE can be easily modified to cope with integer control variables  $x_j$

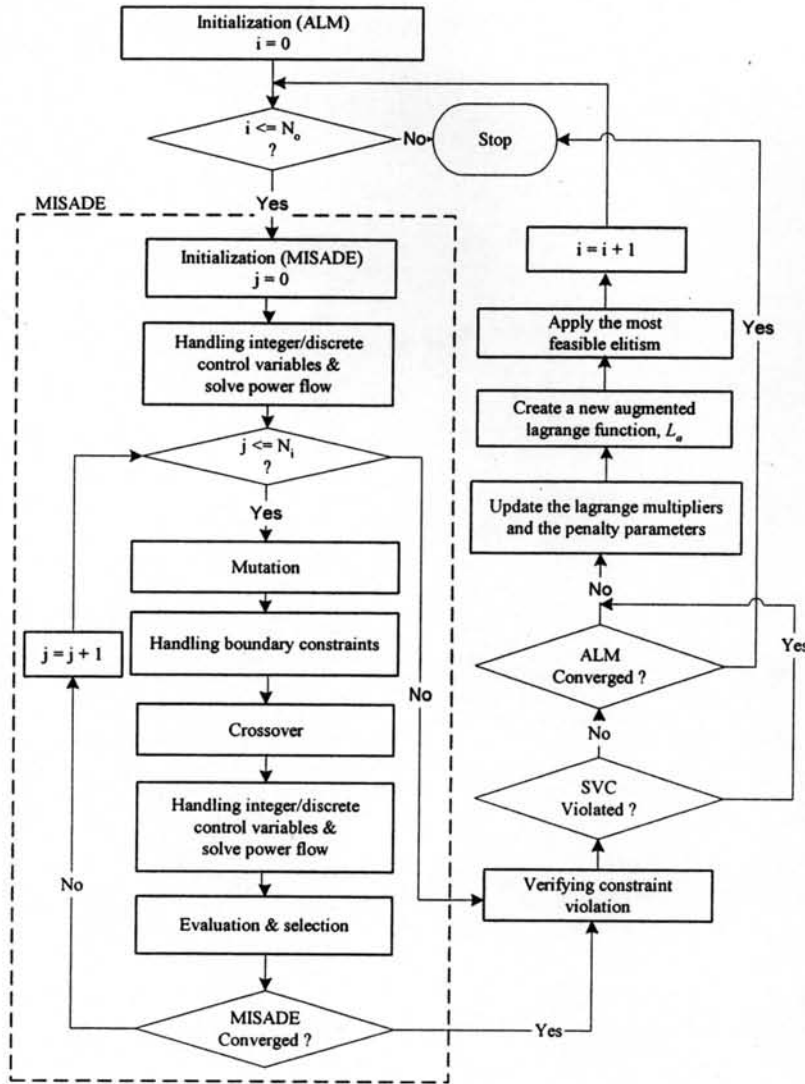


Figure 6.1 Flowchart of MISADE\_ALM-OPF

in a simple manner by transforming the continuous variables to integer variables for power flow calculation in order to determine the state variables, whereas the MISADE itself still works internally as continuous floating point control variables [19].

$$x_{ij}^{(I)} = \begin{cases} INT(x_{ij}), & \text{for power flow calculation} \\ x_{ij}, & \text{otherwise} \end{cases} \quad (6.1)$$

where  $x_{ij}^{(I)}$  is the integer OPF control variable  $i$  of the  $n$ -dimensional parent vector  $X_p$ , and  $INT(\cdot)$  is an integer function for converting a real value to an integer value by truncation. Moreover, the population of the associated integer variables will be initialized using (6.2) instead of (4.25) in chapter 4.

$$x_{ij} = x_{ij,low} + \rho_{ij} \times (x_{ij,hi} - x_{ij,low} + 1) \quad (6.2)$$

Discrete control variables can also be handled in the same way as the integer control variables. Suppose that the discrete control variable  $x_{ij}^{(D)}$  contains  $q$ -elements as in (6.3).

$$x_{ij}^{(D)} = \{x_{ij,1}, x_{ij,2}, \dots, x_{ij,q}\} \quad (6.3)$$

where

$$x_{ij,k} < x_{ij,k+1}, \quad k = 1, \dots, q \quad (6.4)$$

The discrete control variables will be transformed to integer variables of which the boundary constrains are limited to range from 1, 2, ... , $q$ . In the same manner of integer control variable, the discrete value  $x_{ij,k}$  will be used instead of its index  $k$  for power flow calculation.

### 6.2.2 The outer loop iteration

After the inner loop has converged, the outer loop is started by using the ALM method to handle the inequality constraints of the state variables. The details of the outer loop iteration are similar to SADE\_ALM as described in section 4.3.1 of chapter 4.

## 6.3 Numerical Results

The proposed MISADE\_ALM for solving the OPF problems was tested on the IEEE-30 bus test system given in Alsac and Stott [65]. The effectiveness of the proposed algorithm has been tested and compared with other approaches, i.e. TS [9], TS/SA [10], ITS [11], EP [7, 12, 13], and IEP [14] based on different fuel cost characteristics, i.e. 1) quadratic cost curve model, 2) piecewise quadratic cost curve model (multiple fuels), and 3) quadratic cost curve with rectified sine component model (valve-point effects) as described in section 4.5 of chapter 4. Only in phase tap-changing transformers were treated as discrete variables for MISADE\_ALM with allowable tapping ranges of 0.90 – 1.10 and a step size of 0.025, whereas the rest of the control variables were considered as continuous control variables. The parameters of MISADE\_ALM for all test cases used the same setting as described section 4.5 of chapter 4.

### 6.3.1 Case 6.1: The OPF with Quadratic Fuel Cost Function

For this case, bus 1 is the slack bus of the system and the generator cost curves of all the generators are represented by quadratic functions as shown in (3.1). The generator cost coefficients are given in Table 4.1 of chapter 4 [7, 14]. The simulation results are shown in Table 6.1 and the convergence characteristic of SADE\_ALM and MISADE\_ALM is shown in Figure 6.2.

Table 6.1 Comparison of the total generator fuel costs for case 6.1

Algorithm	Fuel Cost (\$/hr.)				Average computational time (minutes)
	Best cost	Average cost	Worst cost	S.D. of cost	
EP [14]	802.907	803.232	803.474	0.226	66.693
TS [14]	802.502	802.632	802.746	0.080	86.227
TS/SA [14]	802.788	803.032	803.291	0.187	62.275
ITS [14]	804.556	805.812	806.856	0.754	88.495
IEP [14]	802.465	802.521	802.581	0.039	99.013
SADE ALM	802.404	802.407	802.411	0.003	15.934
MISADE ALM	802.414	802.446	802.581	0.055	14.970

Note: Based on different computing hardwares

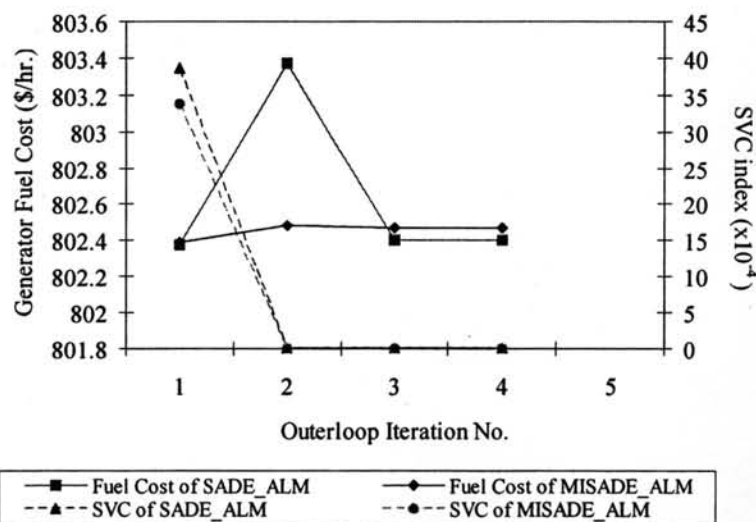


Figure 6.2 Convergence characteristic of SADE\_ALM and MISADE\_ALM for case 6.1

### 6.3.2 Case 6.2: The OPF with Multiple Fuels

In this case, the generator fuel cost curves of generator at bus 1 and 2 are represented by piecewise quadratic functions or multiple fuels using (3.3). Bus 5 is selected as the slack bus of the system to allow more accurate control over units with discontinuities in cost curves [7]. The generator cost coefficients of those two generators are given in Table 4.2 of chapter 4 [7, 14]. The simulation results are shown in Table 6.2 and the convergence characteristic of SADE\_ALM and MISADE\_ALM is shown in Figure 6.3.

Table 6.2 Comparison of the total generator fuel costs for case 6.2

Algorithm	Fuel Cost (\$/hr.)				Average computational time (minutes)
	Best cost	Average cost	Worst cost	S.D. of cost	
EP [14]	650.206	654.501	657.120	2.262	69.865
TS [14]	651.246	654.087	658.911	2.054	88.447
TS/SA [14]	654.378	658.234	662.616	2.788	73.243
ITS [14]	654.874	664.473	675.035	6.888	94.832
IEP [14]	649.312	650.217	651.125	0.555	100.427
SADE_ALM	647.833	648.159	650.049	0.680	17.505
MISADE_ALM	647.836	648.224	650.740	0.892	12.892

Note: Based on different computing hardwares

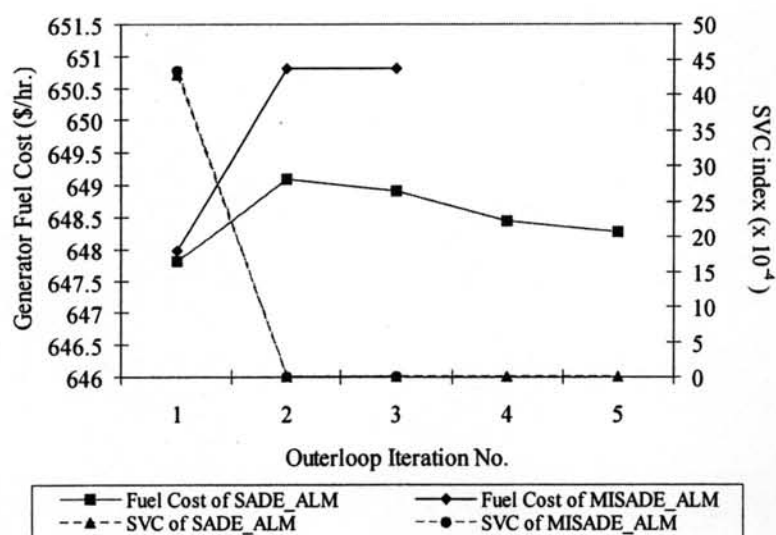


Figure 6.3 Convergence characteristic of SADE\_ALM and MISADE\_ALM for case 6.2

### 6.3.3 Case 6.3: The OPF with Valve-Point Effects

In this case, the generator fuel cost curves of generator at bus 1 and 2 are represented by quadratic functions with rectified sine components or valve-point effects using (3.2). As in case 6.2, bus 5 is selected to be the slack bus of the system. The generator cost coefficients of those two generators are given in Table 4.3 of chapter 4 [7, 14]. The simulation results are shown in Table 6.3 and the convergence characteristic of SADE\_ALM and MISADE\_ALM is shown in Figure 6.4.

Table 6.3 Comparison of the total generator fuel costs for case 6.3

Algorithm	Fuel Cost (\$/hr.)				Average computational time (minutes)
	Best cost	Average cost	Worst cost	S.D. of cost	
EP [14]	955.508	957.709	959.379	1.084	61.419
TS [14]	956.498	958.456	960.261	1.070	88.210
TS/SA [14]	959.563	962.889	966.023	2.146	65.109
ITS [14]	969.109	977.170	985.533	6.191	85.138
IEP [14]	953.573	956.460	958.263	1.720	93.583
SADE ALM	944.031	954.800	964.794	5.371	16.160
MISADE ALM	936.681	953.331	966.338	7.076	14.402

Note: Based on different computing hardwares

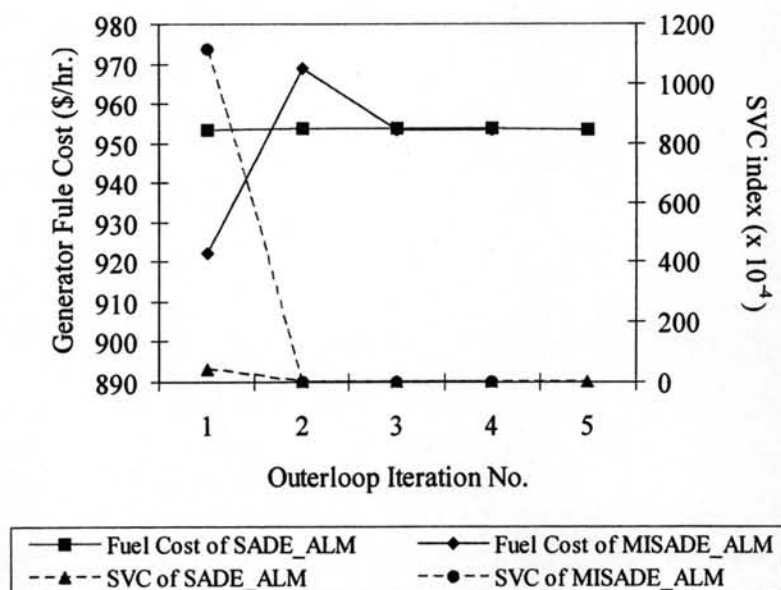


Figure 6.4 Convergence characteristic of SADE\_ALM and MISADE\_ALM for case 6.3



For all test cases, the results from ten test runs of both SADE\_ALM and MISADE\_ALM do not violate any constraints. Tables 6.1 and 6.2 show that the best generator fuel costs of MISADE\_ALM are slightly higher than SADE\_ALM except Table 6.3 where the best generator fuel cost of MISADE\_ALM is significantly lower. In addition, the best and the average fuel costs of SADE\_ALM and MISADE\_ALM are less expensive than those obtained by TS, TS/SA, ITS, EP, and IEP. The optimal values of the best solution given by both algorithms in each case are shown in Table 6.4.

Table 6.4 Optimal solutions given by SADE\_ALM and MISADE\_ALM in each case

Optimal Solution	Case 1		Case 2		Case 3	
	SADE_ALM	MISADE_ALM	SADE_ALM	MISADE_ALM	SADE_ALM	MISADE_ALM
$P_{G1}$ (MW)	176.1522	176.1146	140.0000	140.0000	193.2903	194.9772
$P_{G2}$ (MW)	48.8391	48.8514	55.0000	55.0000	52.5735	52.0580
$P_{G5}$ (MW)	21.5144	21.5096	24.1986	24.2070	17.5458	16.3493
$P_{G8}$ (MW)	22.1299	22.1636	35.0000	35.0000	10.0000	10.0000
$P_{G11}$ (MW)	12.2435	12.2401	18.6439	18.6259	10.0000	10.1640
$P_{G13}$ (MW)	12.0000	12.0000	17.6397	17.6499	12.0000	12.0645
$V_{G1}$ (p.u.)	1.0500	1.0500	1.0500	1.0500	1.0493	1.0213
$V_{G2}$ (p.u.)	1.0381	1.0384	1.0402	1.0405	1.0271	0.9944
$V_{G5}$ (p.u.)	1.0112	1.0119	1.0146	1.0153	1.0081	0.9690
$V_{G8}$ (p.u.)	1.0190	1.0201	1.0255	1.0261	1.0109	0.9871
$V_{G11}$ (p.u.)	1.0911	1.1000	1.0910	1.0971	1.0732	1.0344
$V_{G13}$ (p.u.)	1.0891	1.0863	1.0821	1.0824	0.9634	1.0975
$t_{11}$	1.0556	1.0250	1.0475	1.0250	0.9612	0.9750
$t_{12}$	0.9000	0.9500	0.9139	0.9500	1.0680	0.9000
$t_{15}$	1.0070	1.0000	1.0004	1.0000	1.0118	0.9750
$t_{36}$	0.9420	0.9500	0.9451	0.9500	0.9041	0.9000
Fuel Costs (\$/hr.)	802.404	802.414	647.833	647.836	944.031	936.681

Table 6.5 shows the new tap settings of SADE\_ALM of the optimal solution in Table 6.4 after being modified to the nearest discrete tap. Based on the optimal solutions in Table 6.4 and the new tap setting in Table 6.5, SADE\_ALM violates voltage magnitude of load bus No. 12 by +0.18% for case 6.1, while the generation fuel cost is slightly lower to \$802.402/hr. based on a new 176.1516 MW generation at slack bus No. 1. For case 6.2, SADE\_ALM also violates voltage magnitude of load bus No. 10 and 12 by +0.068% and +0.053%, while the generation fuel cost is slightly increased to \$647.837/hr. based on a new 24.1996 MW generation at slack bus No. 5. For

case 6.3, SADE\_ALM provides the optimal solution without violating any constraints, while the generation fuel cost is slightly increased to \$944.2366/hr. based on a new 17.61 MW generation at slack bus No. 5. Therefore, it can be noticed for case 6.1 and 6.2 that MISADE\_ALM provides the optimal solutions better than SADE\_ALM, while the generation fuel costs of both algorithms are very similar. However, for case 6.3, the generation fuel cost of MISADE\_ALM is significantly lower than SADE\_ALM as shown in Table 6.4. Power flow results of MISADE\_ALM for all test cases are provided in Tables J.1-J.3 in Appendix J.

Table 6.5 New Tap settings of SADE\_ALM after being modified to the nearest discrete taps

Discrete tap	Case 1	Case 2	Case 3
$t_{11}$	1.050	1.050	0.950
$t_{12}$	0.900	0.900	1.075
$t_{15}$	1.000	1.000	1.025
$t_{36}$	0.950	0.950	0.900

#### 6.4 Conclusion

In this chapter, a mixed-integer self-adaptive differential evolution with augmented lagrange multiplier method (MISADE\_ALM) is introduced to solve the OPF problems with a mixture of continuous and discrete control variables. The effectiveness of the proposed algorithms has been tested on the IEEE 30-bus system with different fuel cost characteristics. The MISADE\_ALM is successfully and effectively implemented to find the feasible global or quasi-global optimum of the OPF problems. The proposed MISADE\_ALM shows promising capability for the OPF problems where the optimal settings of discrete control variables are taken into account. In the next chapter, the conclusion and recommendation for future work will be presented.